THE CONTROL OF WIND AND WAVES ON THE ASYMMETRY OF ESTUARINE CURRENTS

Stephen Hunt[1], Karin R. Bryan[2], Julia C. Mullarney[2] and Mark Pritchard[3]

Abstract

Tidal asymmetry is a well-recognised factor controlling the sediment transport and subsequent morphological change in estuaries with peak current strength controlling the transport of coarse bedload sediments and the duration of slack water controlling the deposition of finer suspended load. However, despite this focus on tides as the dominant driver of morphological change, wind waves are capable of exerting a bed shear stress comparable to that created by tides and therefore waves may provide an additional control on long-term morphological form. Here, the interactions between tides, winds and waves and the implications for the net import or export of sediment are explored through the use of a simple idealised hydrodynamic model. Wind and wave climate are shown to affect tidal asymmetry through changes in the magnitudes of peak velocities, with an increase in depth averaged velocity with the wind direction over the intertidal and against the wind direction over the subtidal (through wind-driven circulation patterns), and also through a reduction in the duration of slack water (through wave induced orbital velocities). This result shows that wind and wave climate can shape the long-term morphology of estuaries in environments in which estuary fetch is sufficient enough to allow the generation of waves.

Key words: estuaries, tidal asymmetry, waves, wind, estuarine morphology

1. Introduction

Tidal asymmetry within an estuary arises from the distortion of the tidal wave as it propagates across the adjacent shelf and through the estuary basin. These distortions result in changes to the net sediment transport flux throughout a tidal cycle with ebb (flood) dominance resulting in a net export (import). Understanding the magnitude and direction of this asymmetry helps to predict the future morphological form and stability of the estuary and therefore informs management decisions regarding estuarine habitats and dredging for navigation. The distortion of the tide within an estuary has been related to the estuarine morphological characteristics in a wide range of studies (e.g. Boon and Byrne, 1981, Aubrey and Spear, 1985, Dronkers, 1986, Freidrichs and Aubrey, 1988, Pethick, 1994, Pethick, 1996, Wang *et al*., 2002, Fortunato and Oliviera, 2005, Moore *et al*., 2009, Brown and Davies, 2010, Colby *et al*., 2010). In an estuary with low or absent tidal flats, the width-averaged depth is greater at the crest of the tidal wave (HW) and therefore the crest will travel faster than the trough (LW) over the length of a shallow estuary. The resulting shorter flood duration (and longer ebb duration) results in greater peak speed during the flood. Conversely, in an estuary with high infilled mudflats, the width averaged depth is shallower at the peak of the tidal wave (HW) relative to the trough (LW), in this case the peak will be slowed relative to the trough resulting in a shortening of the ebb phase and therefore ebb dominance (greater speeds on the ebb). These asymmetries in peak velocity primarily influence the residual bedload transport of coarser sediments (sands and gravels) (Dronkers, 1986, Bolle *et al.*, 2010).

[1]Coastal Marine Group, Department of Earth and Ocean Sciences, University of Waikato, Private Bag 3105, Hamilton 3240. New Zealand. sh231@waikato.students.ac.nz
[2]Coastal Marine Group, Department of Earth and Ocean Sciences, University of Waikato.
[3]National Institute of Water and Atmosphere, Hamilton, New Zealand.

The duration of slack water has been identified as an important control on the transport of finer sized sediments (Dronkers, 1986). Slack duration is defined as the time over which the depth-averaged velocity (or equivalent bed shear stress) is lower than the critical threshold for sediment entrainment. Deposition of the sediment onto the seabed is possible during flows below this critical speed.

Meso- and macro-tidal estuaries are commonly assumed to be dominated by these tidal processes. However, wind generated waves can produce bed shear stresses comparable to those created by tides alone (Le Hir *et al.*, 2000) and it has been postulated that wind-waves may be the primary factor controlling sediment suspension flux and erosion over the intertidal regions (de Lange and Healy, 1990, Green *et al.*, 1997, Green *et al.*, 2000, Jannsen-Stedler, 2000, Le Hir *et al.*, 2000). The aim of this research is to quantify the relative importance of wave and wind processes in controlling the net tidal asymmetry in an idealised short basin with well-constrained hypsometric properties.

2. Methods

Flows in a synthetic tidal basin (measuring 5 by 2.5 km) were simulated using the Delft3D hydrodynamic numerical model coupled to the SWAN shallow water spectral wave model. Delft 3D solves the unsteady shallow water equations on a staggered grid and it is used here in depth-averaged barotropic mode (Lesser, 2004). SWAN solves for the evolution of the wave field using the wave action balance equation. The model includes the processes of wind-generation, refraction, nonlinear wave-wave interaction and dissipation through white-capping, bottom-friction and depth induced breaking (Booij *et al*, 1999). The elevation and area of intertidal regions can be described in terms of hypsometry which defines the estuarine basin area above a given height plane (Strahler, 1952, Boon, 1975, Boon and Byrne, 1981, Eiser and Kjerfve, 1986, Oertel, 2001, Wang *et al.*, 2002, Moore *et al.*, 2009, Yu *et al*, 2012). Here, the basin hypsometry was defined by the following equation (Boon and Byrne, 1981):

$$a/A = G/(r + G[1-r]) \quad (1)$$

and

$$G = (1-h/H)^{\gamma} \quad (2)$$

where h is the height above minimum basin elevation, A is the maximum basin area, a is the basin area lying above height h, H is the height between lowest and highest basin elevation. The empirical parameter $r = 0.01$ represents the basin curvature based on the slope at the point of inflection (Boon and Byrne, 1981). The area below the hypsometric curve (γ) corresponds to the volume of sediment in the basin and hence provides an indication of the maturity (or amount of sediment infill) within the estuary. Larger values of γ correspond to reduced amounts of sediment within the intertidal area, with the majority of the intertidal below mean sea level. Hence, larger values are characteristic of the morphology associated with young, flood-dominant estuaries (Dronkers, 1986, Pethick, 1994, Pethick, 1996). Conversely, smaller values of γ are typical of ebb dominant estuaries and correspond to enhanced volumes of intertidal sediment, with tidal flats lying above mean sea level (Dronkers, 1986, Pethick, 1994, Pethick, 1996).

To assess the interaction of tides, wind and waves two sets of model runs were executed, firstly forced by tides only (Delft3D hydrodynamic module only) and secondly with forcing from wind, waves and tides (Delft3D coupled to SWAN). The model was forced by an astronomically forced M_2 tide (2m amplitude) at the seaward boundary which was situated 5km away from the estuary mouth (Figure 1). Spatially-uniform and constant winds of 5 and 10m/s in both a easterly (seaward) and westerly (landward) direction were applied at the water surface for the duration of the simulation. A uniform bottom friction Manning coefficient of 0.035 was applied throughout the model. The model grid

resolution was 50m and the timestep was 1 minute. Each scenario was run for 5 tidal cycles, with output variables written to file every 2 minutes for the entire domain. Simulations were started from rest with a uniform sea surface at mean sea level throughout the domain and runs were allowed to evolve to a cyclically steady state. The results from the transitional period of the first tidal cycle were discarded. We present results from an unfilled estuary (γ=4.0, Equation 2) in detail, the morphology of this estuary is schematically represented in Figure 2. Flows and water levels have been analysed for two indices of tidal asymmetry: (i) the maximum peak velocity, which controls the transport of coarse sediment as bedload and (ii) the slack duration, which controls the deposition and transport of fine suspended sediments.

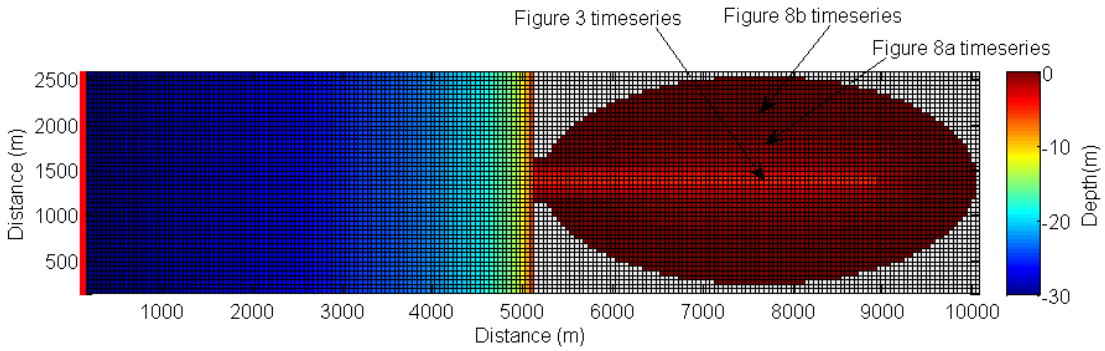

Figure 1. Numerical model grid and bathymetry. The model is forced at the single open boundary on the left hand side of the domain (thick red line). The locations from which the time series shown in Figures 3, 8a and 8b are indicated by the arrows.

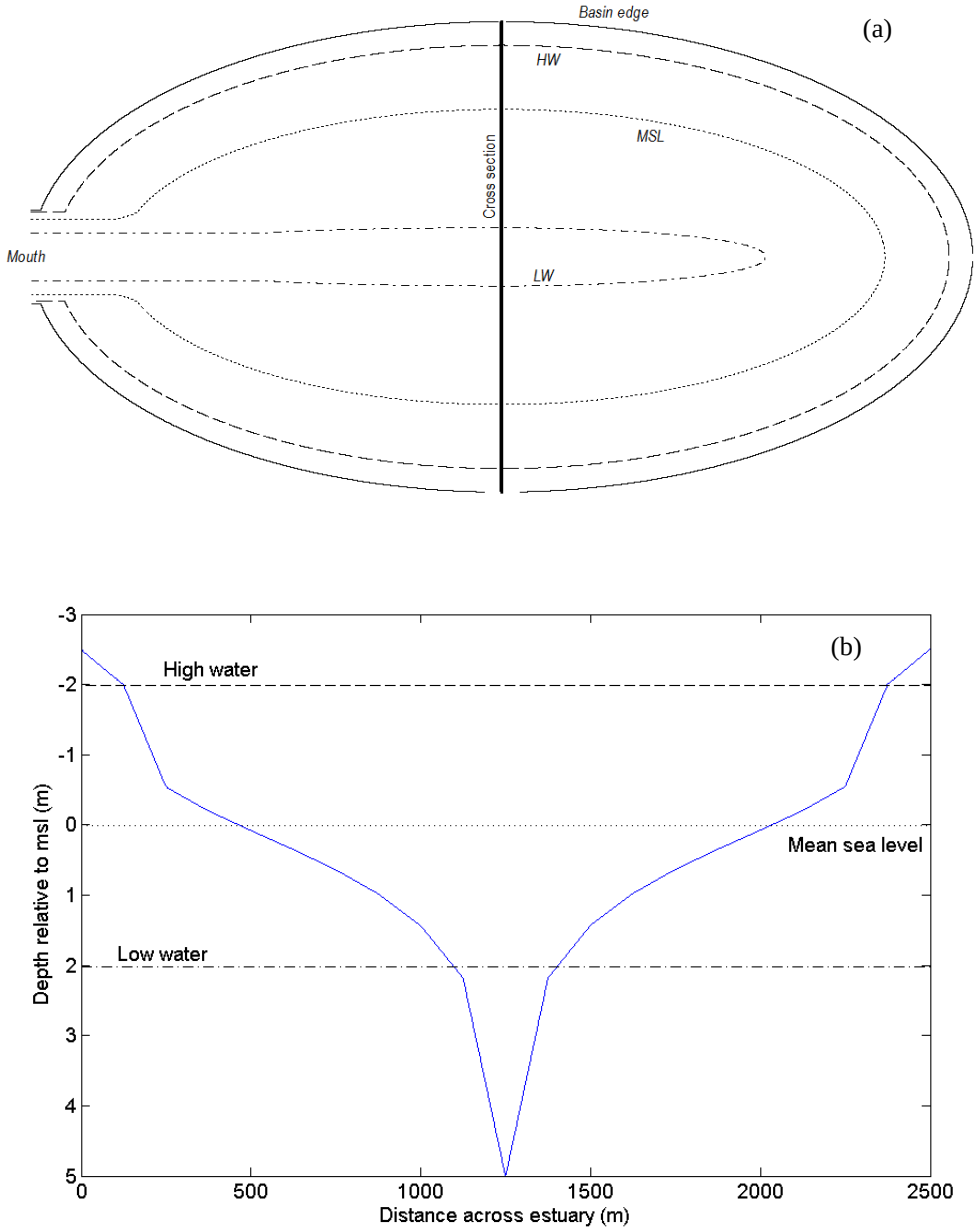

Figure 2. Schematic representation of the unfilled (γ=4.0) estuary: (a) showing overhead view and (b) side view along the central North-South cross-section marked in (a). Low water, mean sea level and high water are shown to illustrate the intertidal form.

3. Results

3.1 *Tide only forcing*

Bottom friction modifies the shape of the tidal wave as it enters the estuary, resulting in the timing of the trough (LW) slowing relative to the timing of the peak (HW) (Figure 3). Mass conservation leads to greater velocities during the flood and hence the estuary is classified as flood dominant in terms of peak velocity.

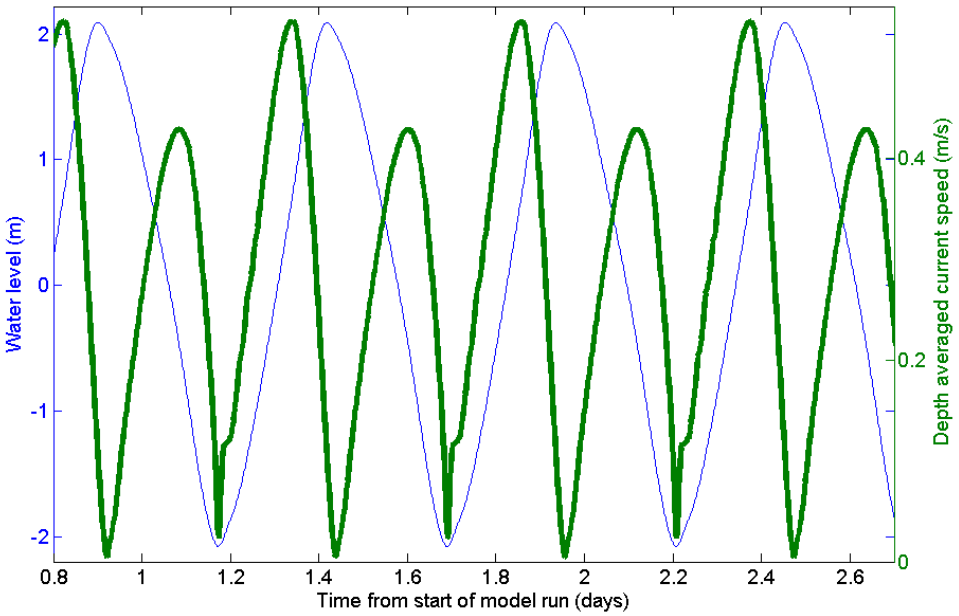

Figure 3. Example timeseries of water levels (thin blue line) and depth averaged velocities (thick green line) taken from the central subtidal area of the model.

The distortion of the tidal wave occurs due to non-linear interaction with the bed and the generation of sub-harmonics as the tidal wave enters shallower water (Friedrichs and Aubrey, 1988). Hence, the amount of modification and resultant direction of peak velocities can be quantified through a comparison of the M_2 and M_4 tidal constituents. A direct measurement of non-linear distortion is given by the ratios of the amplitudes:

$$Distortion\ magnitude = M_4\ amplitude\ /\ M_2\ amplitude \tag{3}$$

whereby a ratio of 0 indicates a completely undistorted tide and a ratio > 0.01 indicates significant distortion of the tidal wave (Friedrichs and Aubrey, 1988).

The direction of the asymmetry (flood or ebb) can be defined by calculating the phase of M_4 constituent relative to that of the M_2 constituent as follows:

$$Relative\ phase = 2M_2\phi\text{-}M_4\phi \tag{4}$$

A relative phase between 0° and 180° indicates that the duration of the ebb tide is longer than the duration of the flood tide and therefore the tide will be flood dominant. Values of relative phase greater than 180° indicate that the duration of the ebb tide is shorter than the duration of the flood tide and therefore the tide can be considered ebb dominant. Tidal constituents for subtidal regions were analysed using the T-tide matlab package (Pawlowicz *et al.*, 2002).

For the tide only forcing, considerable distortion (distortion magnitude > 0.01) occurs throughout most of the subtidal channel (Figure 4a), except for the region close to the estuary mouth. The distortion increases as the tide propagates through the estuary with maximum distortion occurring at the landward end of the estuary. Both the M_2 to M_4 phase difference (Figure 4b) and depth averaged velocities (Figure 5) indicate flood dominance (peak velocities during flood tide) throughout the majority of the subtidal regions (Figure 4b). The occurrence of peak velocities during the flood tide suggests a regime in which there is a net import of coarse bedload sediments.

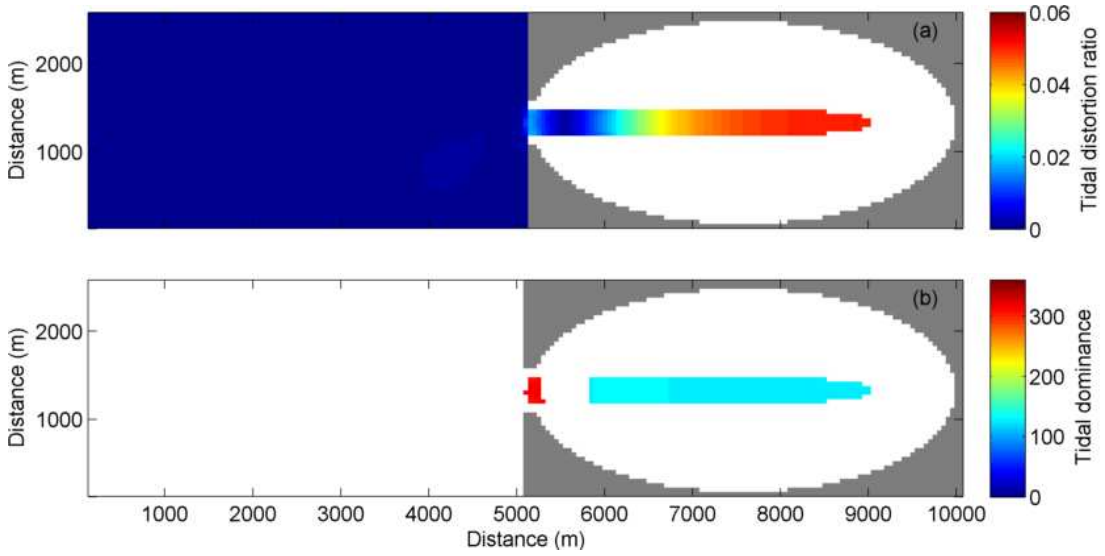

Figure 4. Plan view of distortion magnitude (a) (equation 3) and resultant direction of peak-velocity from distortion (b) (equation 4). Figure 4b only shows phase difference in subtidal areas where the distortion is significant (>0.01). Simulations for an infilled mature estuary ($\gamma = 4$) and tide only forcing. Grey areas denote land.

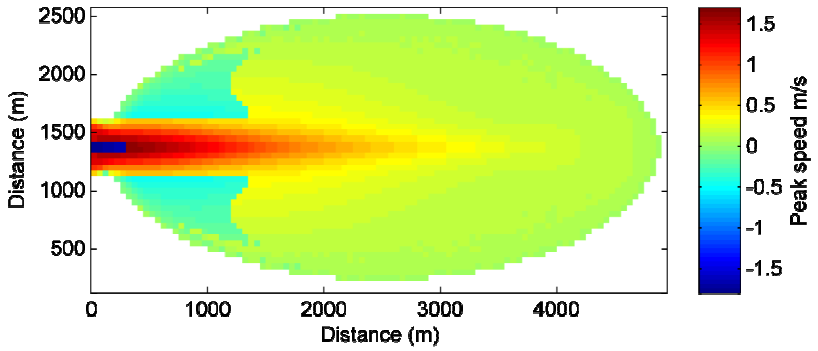

Figure 5. Peak velocity magnitudes from simulations with tide-forcing only. Negative (positive) values indicate that the peak velocity occurs during the ebb (flood) phase of the tide.

Next, we examine the slack duration at high water to investigate the potential for sediment deposition over the intertidal flats. Although duration of slack water decreases slightly on the intertidal owing to the shorter periods of submergence, this is largely offset by lower velocities resulting in a net increase in slack water duration over much of the intertidal region. The duration of slack water is shown in Figure 6 relative to a bed shear stress capable of entraining a sediment particle measuring 100 micron.

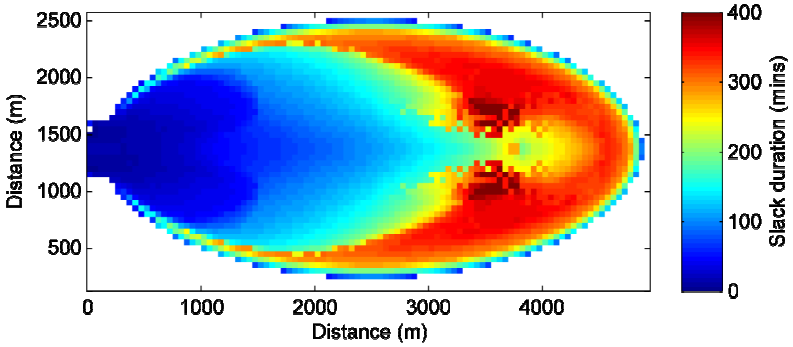

Figure 6. Slack water duration in minutes at high water defined as the amount of time that bed shear stress drops below the entrainment threshold for a sediment particle of 100 micron.

3.2 *Tide, wind and wave forcing*

For the flow simulations forced by both wind and tide, the ratios of tidal constituents (not shown) show no discernible difference from the simulations without wind forcing (Figure 4). Thus, any changes in the tidal asymmetry resulting from the presence of wind and waves can be attributed to their direct influence on the flow patterns rather than the distortion of constituents. The distribution of peak velocities throughout the estuary was examined using simulations with 5 m/s and 10 m/s seaward (easterly) wind (Figure 7a and 7b) and the 5 m/s and 10 m/s landward (westerly) wind (Figure 7c and 7d).

In all cases, the addition of wind forcing changes the flow magnitudes over the intertidal areas; depth-averaged velocities were found to increase in the direction of the prevailing wind, so that flood currents were enhanced during a landward wind and ebb currents were enhanced under a seaward wind. For tidal asymmetry (assessed from peak velocities), moderate wind speeds (5m/s) lead to an increase in flood dominance during a landward breeze and an increase in ebb dominance during an seaward breeze. However, for larger wind speeds (10m/s) both seaward and landward breezes increase the magnitude of ebb dominance. This counterintuitive result for landward winds can be explained by the generation of large return currents in the upper estuary (Figure 7d).

Within the subtidal region the pattern of asymmetry is opposite to that over the intertidal, such that the increase in peak-velocity magnitude is against the prevailing wind direction, *i.e.* we observe an increase in flood dominance with a seaward wind and an increase in ebb dominance with a landward wind (Figure 7). Two factors contribute to this pattern; firstly return flows at the ends of the estuary result in enhanced subtidal depth-averaged velocities in the opposite direction to that observed over the intertidal. Secondly, the influence of the wind is felt over a smaller proportion of the water column in the deeper subtidal regions, so depth-averaged flow speeds decrease in the subtidal, whilst the depth-averaged flow speeds increase over the intertidal (owing to mass conservation through the estuarine cross section).

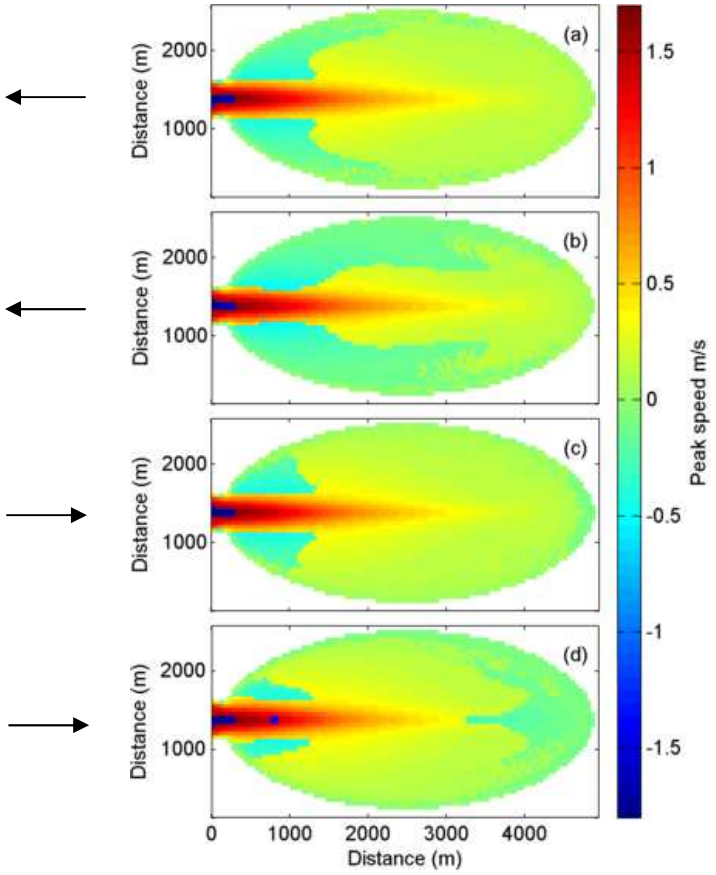

Figure 7. Peak velocity magnitudes for 5 (a) and 10m/s (b) seaward wind and 5 (c) and 10m/s (d) landward wind, negative (positive) values indicate that the peak velocity occurs during the ebb (flood) phase of the tide. Wind direction is indicated with arrows.

The most dramatic impacts of the addition of wind are observed in the slack water duration. Wind-forced waves predominantly affect the seabed sediments through wave orbital velocities. Although these orbital velocities only result in a small net transport, they are capable of suspending sediments, which can then be transported by mean currents to less hydrodynamically-active areas for deposition. These orbital velocities increase with wave height, wave period and wavelength and therefore are directly proportional to the available fetch and wind speed. Within an estuary, the greatest potential for wave generation is at high water when the largest fetch is available. However, due to the attenuation of wave orbital velocities with increasing depth, the maximum impact of the orbital velocities will occur at a point at which there exists a balance between the available fetch for wave generation and sufficiently shallow water depths that allow the orbital velocities to reach the seabed (Green *et al.*, 1997). As sediment entrainment will occur as a result of both tidal and wave currents, we consider the resultant hydrodynamic forcing on the seabed as a combined bed shear stress from both waves and currents: the duration that this maximum combined bed shear stress (*i.e.* both tide and wind forcing scenarios) was not sufficient to entrain a sediment measuring 100 micron is shown in Figure 8.

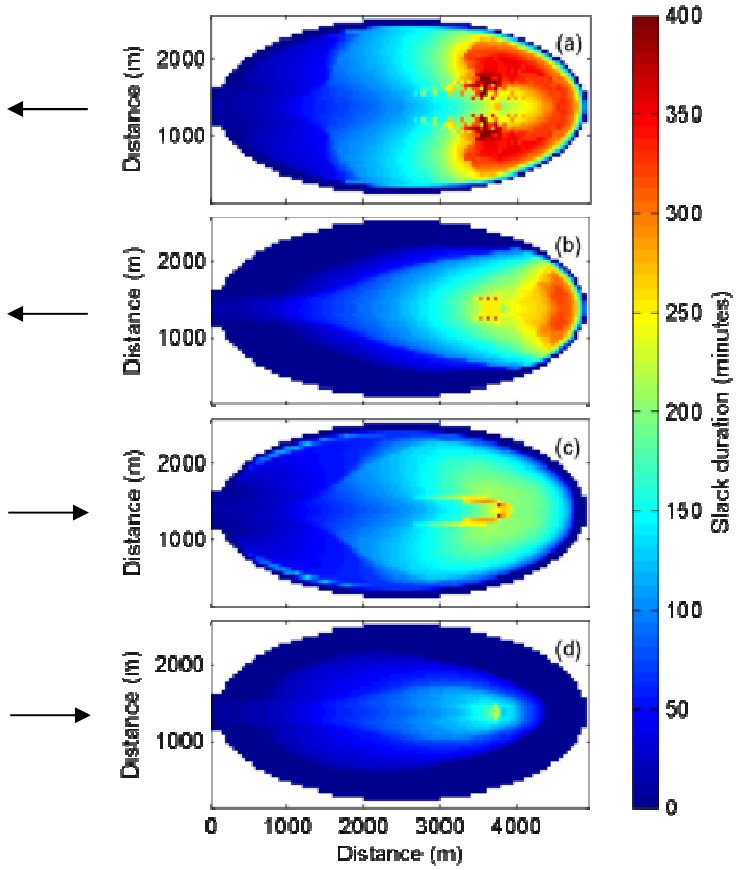

Figure 8. Slack duration as a result of combined maximum bed shear stress in minutes under a 5m/s (a) and 10m/s (b) seaward wind and a 5m/s (c) and 10m/s (d) landward wind. Wind direction is indicated with arrows.

Figure 8 illustrates the reduction in slack duration with larger wind speeds (and therefore larger wave height and orbital velocities). The dependence of the potential for deposition on the depth of the water column is particularly striking. Within the shallower fringing parts of the basin, the attenuation of wave orbital velocities is minimal even at high water slack, and the 'stirring' from waves prevents any deposition of sediment. This lack of deposition around the estuary margin is consistent with the recorded band of highly turbid water (termed the turbid fringe) attributed to waves breaking in shallow water within Manakau Harbour, New Zealand (Green *et al.*, 1997 and 2000). Within the deeper intertidal areas the orbital velocities are attenuated at high water, reducing their effect on the bed. Hence, waves exert their main influence at mid-tide when the fetch is sufficient for wave generation and yet the depth is still shallow enough for the orbital velocities to reach the seabed. Consequently, wave orbital velocities enhance the bed shear stress during maximum tidal currents, which results in a peak combined bed shear stress at mid tide and an enhancement of the net transport from peak tidal velocity with a slack water period at high water. This pattern of wave-current interaction is shown for a shallow (Figure 9a) and deep (Figure 9b) intertidal region as a timeseries under a 10m/s westerly wind speed. Within subtidal areas the water is too deep for orbital velocities to impact on the seabed regardless of wind speed.

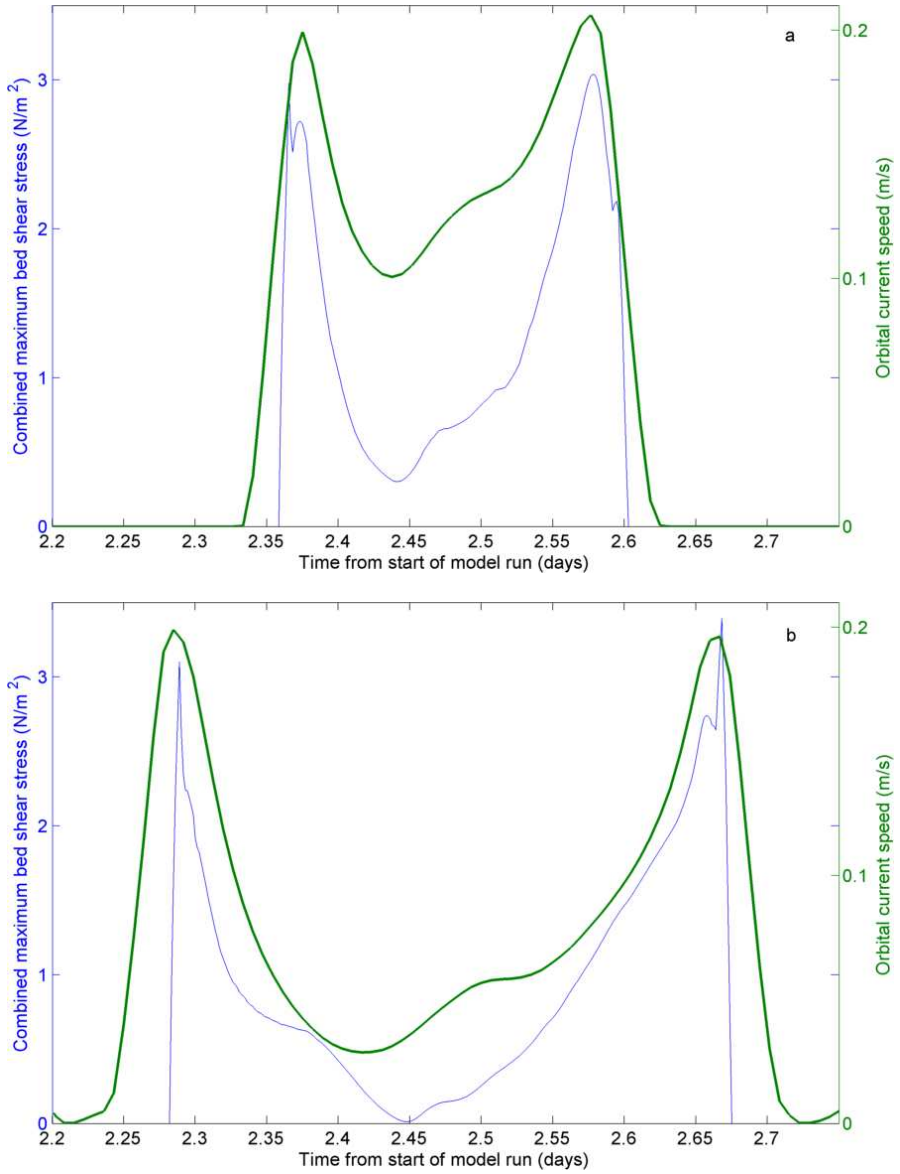

Figure 9. Wave orbital current speed (thick green line) and resultant bed shear stresses (thin blue line) shown for a shallow (a) and deep intertidal area (b).

4. Discussion

The patterns of tidal asymmetry indicate a net import of sediment and subsequent accretion of the intertidal area, when only tide forcing is applied to the model. The asymmetry of peak velocities is stronger on the flood due to the distortion of the tidal wave resulting in a net flux of sediment into the estuary. This import of sediment is reinforced by the long period of slack duration which allows the deposition of imported sediment onto the intertidal flats.

Under windy conditions (10 m/s) the wind-driven circulation in both landward and seaward directions tends to favour seaward peak velocities owing to both changes in the circulation in the subtidal

channel and wind assisted transport over the intertidal areas. Although windy conditions do not change the overall net flux of sediment, the ebb dominance is enhanced, thereby reducing the amount of sediment imported over a tidal cycle. Waves do not greatly impact on the large-scale circulation patterns, but the wave orbital velocities instead directly influence bed shear stresses. The overall affect of waves is to reduce the duration of depositional conditions on the intertidal both through a reduction in slack duration (preventing sediment deposition) and an increase in bed shear stress (causing further erosion). The impact of the waves is negligible in the subtidal channel, owing to the depth attenuation of orbital velocities; hence the flows in these regions are dominated entirely by tidal processes. However, suspended sediment levels within the subtidal channel will still be influenced by the sediment entrainment on the intertidal. Fieldwork in Manakau Harbour (Green *et al.*, 2000) noted that sediment entrained on the shallow edge of the intertidal (the turbid fringe) during wave events was flushed into the main channel on the ebbing tide and subsequently dispersed. The fate of the sediment could not be determined but the excess turbidity dispersed within a day or so of the initial suspension.

This pattern of intertidal accretion under tidal conditions and erosion where the fetch of the estuary is sufficiently long to allow the generation of wind waves has been hypothesised in field studies (Green *et al.*, 1997, Jannsen-Stedler, 2000). Even small wind waves have been found to be capable of transporting small amounts of fine sediment (Green, 2011). The significance of wind and waves on the sediment transport regime has implications for the understanding of estuarine dynamics. Many areas of the world experience regular, repeatable patterns of wind direction and speed over either monthly (e.g. seasonal patterns), interannual (e.g. El Niño /La Niña) or even daily (sea /land breezes) timescales. In locations in which the fetch axis is aligned with dominant wind directions, the resultant morphology may depend on the wind climate as well as the tidal regime. Consequently changes to the wind regime as a result of climate change may have significant implications for estuarine stability, with reductions in wave height leading to intertidal accretion and increases in wave height enhancing intertidal erosion. However, inherent uncertainties in future climate change predictions will also result in uncertainties in the prediction of the change in estuarine environments. These uncertainties associated with the wind-forced patterns are in stark contrast to the wholly predictable patterns of tidal height which can be reliably hindcast and forecast.

5. Conclusions

This paper presents preliminary results from an idealised modelling study investigating the impacts of wind and wave forces on tidal asymmetry within a small macro-tidal basin. Although this study is presently only limited to one basin type, some interesting and complex relationships between tides, winds and waves were revealed. Overall the idealised model indicated intertidal accretion under tides. This accretion occurs as peak velocities take place during the flood tide, thus favouring a net import of sediments and a slack duration at high water during which sediments can settle out of suspension. When wind and waves are included within the model, the amount of intertidal accretion is reduced. This reduction occurs in part due to changes to the patterns of circulation within the estuary which increase the strength of ebb currents but more significantly as a result of the stirring by the wave orbital velocities during high water slack, which prevents the deposition of sediments.

The apparent importance of the wind and wave climate in shaping the patterns of sediment deposition and erosion (even under relatively low wind speeds) suggests that wind and waves can contribute to the form of the resultant estuarine morphology in estuaries where the fetch favours the predominant wind direction. This result shows the importance of including the forcing from tides, winds and waves when predicting future changes in estuarine morphology.

References

Aubrey, D.G. and Spear, P.E. 1985. A study of Non-linear Tidal Propogation in shallow Inlet/Estuarine Systems Part I: Observations. *Estuarine, Coastal and Shelf Science*, 28, 185-205.

Bolle, A., Wang, Z.B., Amos, C. and De Ronde, J. 2010. The influences of changes in tidal asymmetry on residual sediment transport in the Western Scheldt. *Continental Shelf Research*, 30, 871-882.

Booij, N., Ris, R.C. and Holthuijsen, L.H. 1999. A third-generation wave model for coastal regions. 1. Model description and validation. *Journal of Geophysical Research*, 104, 7649-7666.

Boon, J.D. 1975. Tidal discharge asymmetry in a salt marsh drainage system. *Limnology and Oceanography*, 20(1), 71-80.

Boon, J.D. and Byrne, R.J. 1981. On basin hypsometry and the morphodynamic response of coastal inlet systems. *Marine Geology*, 40, 27-48.

Brown, J.M. and Davies, A.G. 2010. Flood/ebb tidal asymmetry in a shallow sandy estuary and the impact on net sand transport. *Geomorphology*, 114, 431-439.

Colby, L.H., Maycock, S.D., Nelligan, F.A., Pocock, H.J. and Walker, D.J. 2010. An investigation into the effect of dredging on tidal asymmetry at the River Murray Mouth. *Journal of Coastal Research*, 26 (5), 843-850.

De Lange, W and Healy, T. 1990. Wave Spectra for a Shallow Meso-Tidal Estuarine Lagoon: Bay of Plenty, New Zealand. *Journal of Coastal Research*, 6, 189-199.

Dronkers, J. 1986. Tidal asymmetry and estuarine morphology. *Netherlands Journal of Sea Research*, 20, 117-131.

Eiser, W.C. and Kjerfve, B. 1986. Marsh Topography and Hypsometric Characteristics of a South Carolina Salt Marsh Basin. *Estuarine, Coastal and Shelf Science*, 23, 595-605.

Fortunato, A.B. and Oliveira, A. 2005. Influence of intertidal flats on tidal asymmetry. *Journal of Coastal Research*, 21, 1062-1067

Friedrichs, C.T. and Aubrey, D.G. 1988. Non-linear tidal distortion in shallow well-mixed estuaries: a synthesis. *Estuarine, Coastal and Shelf Science*, 27, 521-545.

Green, M.O. 2011. Very small waves and associated sediment resuspension on an estuarine intertidal flat. *Estuarine, Coastal and Shelf Science*, 93, 449-459.

Green, M.O., Black, K.P. and Amos, C.L. 1997. Control of estuarine sediment dynamics by interactions between currents and waves at several scales. *Marine Geology*, 144, 97-116.

Green, M.O., Bell, R., Dolphin, T.J. and Swales, A. 2000. Silt and sand transport in a deep tidal channel of a large estuary (Manakau Harbour, New Zealand). *Marine Geology*, 163, 217-240.

Janssen-Stedler, B. 2000. The effect of different hydrodynamic conditions on the morphodynamics of a tidal mudflat in the Dutch Wadden sea. *Contenental Shelf Research*, 20, 1461-1478.

Le Hir, P., Robets, W., Cazaillet, O., Christie, M., Bassoullet, P. and Bacher, C. 2000. Charaterization of intertidal flat hydrodynamics. *Continental Shelf Research*, 20, 1433-1459.

Lesser, G.R., Roelvink, J.A., van Kester, J.A.T.M. and Stelling, G.S. 2004. Development and validation of a three-dimensional morphological model. *Coastal Engineering*, 51, 883-915.

Moore, R.D., Wolf, J., Souza, A.J. and Flint, S.S. 2009. Morphological evolution of the dee Estuary, Eastern Irish Sea, UK: A tidal asymmetry approach. *Geomorphology*, 103, 588-596.

Oertel, G.F. 2001. Hydro-Hypsographic and Hydrological Analysis of Coastal Bay Environments, Great Machipongo Bay, Virginia. *Journal of Coastal Research*, 17, 4, 775-783.

Pawlowicz, R., Beardsley, B. and Lentz, S. 2002. Classical tidal harmonic analysis including error estimates in MATLAB using T_TIDE. *Computers and Geosciences*, 28, 929-937.

Pethick, J.S. 1994. Estuaries and wetlands: function and form. In: Falconer, R.A. and Goodwin, P. (eds). *Wetland Management.* London, Thomas Telford Services Ltd.

Pethick, J.S. 1996. The geomorphology of mudflats. In: Nordstrom, K.F. and Roman, C.T. (eds.) *Estuarine Shores: Evolution, Environments and Human Alterations.* Chichester: Wiley.

Strahler, A. N. 1952. Hypsometric (area-altitude) analysis of erosional topography. *Geological Society of America Bulletin*, 63, 1117-1142.

Wang, Z.B., Jeuken, M.C.J.L., Gerritsen, H., de Vriend, H.J. and Kornman, B.A. 2002. Morphology and asymmetry of the vertical tide in the Westerschelde estuary. *Continental Shelf Research*, 22, 2599-2609.

Yu, Q., Wang, Y., Flemming, B. and Gao, S. 2012. Modelling the equilibrium hypsometry of back-barrier tidal flats in the German Wadden Sea (southern North Sea). *Continental Shelf Research*, 49, 90-99.